Surface Roughening in Electrodeposited Nickel Films on ITO Glasses at a Low Current Density

M. Saitou, A. Makabe and T. Tomoyose

Dept. of Mechanical Systems Engineering, University of the Ryukyus, 1 Senbaru Nishihara-cho, Okinawa, 903-0213 Japan

We have studied the kinetic surface roughening of nickel films electrodeposited on ITO glasses at a low current density using atomic force microscopy, electron and X-ray diffraction. The AFM images of the nickel films exhibited the scaling relations represented by the growth exponent $\beta=0.78\pm0.03$ and the roughness exponent $\alpha=0.96\pm0.04$ that is in good agreement with the prediction by the diffusion-driven growth model. Electron and X-ray diffraction revealed a preferred growth orientation of the electrodeposited nickel films, which gives an explanation for the growth exponent β greater than 1/2.

Keyword: Nickel; Electrochemical methods; Surface roughening; Surface morphology; Atomic Force Microscopy; X-ray diffraction; Electron-solid diffraction

In order to understand growth processes as a good example of dynamical scale invariance [1-3], many theoretical and experimental investigations into the kinetic surface roughening in thin films grown by deposition have been made and revealed the simple scaling relation that the interface width obeys $w(L,t) \sim L^{\alpha} f(t/L^{\alpha/\beta})$ where L indicates a system size at time t, α the roughness exponent and β the growth exponent. These exponents α and β determine universality classes characterizing the scaling behavior of the growth mechanisms, irrespective of experimental details and imply the presence of the self-affine surface morphology. Positive values of β indicate that unstable interface fronts develop with time. For example, for the diffusion-driven model of the growing surface, the time evolution of the surface height $h(\mathbf{r},t)$ on basis of symmetry principles has the form [4],

$$\partial h / \partial t = -\kappa \nabla^4 h + \lambda \nabla^2 (\nabla h)^2 + F + \eta, \qquad (1)$$

where κ and λ are constants, F is the average number of particles arriving at r, which does not affect the scaling exponents, and η reflects the random fluctuations in the deposition process. The exponents α and β are obtained theoretically for two interesting cases in growth on two-dimensional substrates: for $\lambda=0$ and $\kappa\neq0$, $\alpha=1$ and $\beta=1/4$; for $\lambda\neq0$ and $\kappa\neq0$, $\alpha=2/3$ and $\beta=1/5$.

Unfortunately there have been very few reports about the scaling behavior of electrodeposited nickel thin films. Electrodeposition of nickel films is of technological importance and nickel metals are well known for ones that are easy to form passive films [5]. Electrodeposits at a low current density generally yield self-affine deposits [6,7], which are dominated by local-effects not but by non-local effect such as diffusion and electromigration of ions in electrolytes. In this study, nickel films were electrodeposited on ITO glasses for 80-800sec at a very low current density in a still nickel sulfamate bath. Atomic force microscopy (AFM), electron and X-ray diffraction were employed to characterize the surface morphology and crystallographic orientations of the electrodeposited nickel films. The purpose of this study is to evaluate the scaling exponents of the nickel surface electrodeposited at a low constant current density and to discuss about the growth exponent β larger than 1/2 in light of the preferred growth orientation.

The substrates prepared were ITO glasses (sheet resistivity 6Ω/) with the rms roughness of 1.2nm cleaned by a wet process. The ITO glass plate for cathode electrodes and the nickel films for anode electrodes were located parallel in a still bath containing (g/l): nickel sulfamate, 600; nickel chloride, 5; and boric acid, 40. The bath

was maintained at pH 4, the temperature of 323 K and a very low fixed current density of 2mA/cm^2 that was chosen in order that nickel electrodeposition could be dominated only by local effects. In fact, the cathode potential measured at the current density by a Luggin capillary as a reference electrode was 0.41V(SCE) in the linear region of the Butler-Volmer equation [8]. The samples were scanned in air with AFM with a resolution of 512x512 pixels. The AFM images with different scan regions of 500x500, 1000x1000 and 2000x2000nm^2 were used for the calculation of the scaling exponents.

In order to determine the exponents α and β from the AFM images, we calculate the interface width w(L,t) defined by the rms fluctuation in the surface height and the height-difference correlation function G(r,t), which have the forms [1,9],

$$w(L,t)=\langle[h(r,t)-\langle h\rangle]^2\rangle^{1/2} \propto t^{\beta}, \quad (2)$$

$$G(r,t)=\langle[h(r+r_1,t)-h(r_1,t)]^2\rangle_{r1} \propto \rho(t)r^{2\alpha}, \text{ for } r<<\xi, \quad (3)$$

$$\xi \propto t^{1/z}, \quad (4)$$

where $\langle...\rangle$ is the spatial average over the measured area, ξ the correlation length, $\rho(t)$ the average local slope of mounds[10-12] given by $\langle(\nabla h)^2\rangle^{1/2}$ and the dynamic exponent $z=\alpha/\beta$.

Fig.1 shows the AFM images of the nickel surface with a region of 2000x2000nm electrodeposited at a low current density of 2mA/cm^2 for 200, 500 and 800sec. The vertical scale of each image with a resolution of 512x512 pixels was magnified by a factor of 3.6 in order to enhance viewing. Nickel morphology appears to be continuous mounds that become larger as the process proceeds.

Fig.2 shows a log-log plot of G($\mathbf{r}$,t) vs the lateral distance r for the electrodeposited nickel films. It can been seen that G($\mathbf{r}$,t) increases linearly with r and reaches a saturated value. The plateau point in Fig.2 corresponds to the correlation length ξ, which is equal to an average mound size formed on the surface. These curves at small length scales do not collapse onto a single curve, i.e., indicate an anomalous behavior predicted by Eq.(3). This arises from the time-dependence of the average local slope of the mounds $\rho(t)$ in the linear diffusion model . The similar anomalous behavior has been already reported by Yang et al.[11] and Jeffries at al.[12]. We obtain an average value of the roughness exponent $\alpha=0.96\pm0.04$ independent of the electrodeposition time and almost consistent with that predicted by the diffusion-driven model for $\lambda=0$ and $\kappa\neq0$.

Fig.3 shows w(t) vs the growth time t in a log-log scale, which gives the growth exponent $\beta=0.78\pm0.03$, far from the prediction by the diffusion-driven model. In general the theoretical value of β is 1/2 and under [1,2]. The experimental value of β >1/2 [7,13,14] has been tentatively explained by the Schwoebel effect [15,16] and shadowing [1]. In order to explain the experimental value of β larger than 1/2 in this study, we made attempts to determine crystallographic orientations of the mounds grown on the ITO glass by using electron and X-ray diffraction. Specimens for TEM examination were prepared by dipping up the electrodeposited nickel film on the copper mesh in HF solution. Fig.4 (a) shows a typical electron diffraction pattern of the nickel film at electrodeposition time 440sec, which indicates that the continuous (111) ring has a stronger intensity than the spotty (200) ring. Fig4.(b) shows a typical X-ray diffraction pattern of the nickel film grown for 1500sec, which the type {111} planes also has a much stronger intensity than the type {200} planes. It can be seen from these results that the mounds grown on the ITO glass have the preferred crystallographic growth orientation [111]. Moreover, Fig.5 shows the AFM image of the mounds with a size of 500x500nm^2 that comprise preferred crystallographic planes. Hence the atom diffusivity in the direction normal to the substrate will become different from that parallel to the substrate. In the similar way to the Schwoebel effect, this brings about a larger β in our system.

We evaluate the dynamic exponent z not by the values of α and β obtained from Figs.2 and 3 but by the slope of the correlation length ξ vs time t in a log-log scale. The correlation length ξ was determined from the plateau points as shown in Fig.2. The slope 1/z in Eq.(4) becomes 0.80 ± 0.08, which is in good agreement with β/α obtained from Fig.2 and Fig.3. The dynamic exponent z in this study is 1.25 by far less than 4 predicted by the linear diffusion-driven model.

Next we calculate the average slope of the mounds and its time-dependence from the AFM images. The average slope is given by $(C(0))^{1/2}/r_c$[17,18], here C(r) is the height-height correlation function defined by $C(r)=\langle h'(r,t)h(0,t)\rangle$ where $h'(r,t)=h(r,t)-\langle h\rangle$,and r_c is the average mound radius determined by the position of the first zero of C(r). We have the average slope 0.43 ± 0.07 approximately independent of the electrodeposition time. This may be related to the preferred crystallographic growth orientation [111]. Johnson et al. [19] showed that singular surfaces are unstable and develop large scale mounds with their constant slopes. Anyway we need a theory that makes it possible to give the growth exponent β larger than 1/2 beyond the surface diffusion-driven growth model.

In summary, the scaling exponents for the electrodeposited nickel films on the ITO

glasses were determined by the surface measurements of AFM and compared with the theoretical values of the surface diffusion-driven growth model. The roughness exponent $\alpha=0.96\pm0.04$ is in good agreement with the value of the model for $\lambda=0$ and $\kappa\neq0$. The growth exponent $\beta=0.78\pm0.03$, much larger than the prediction by the surface diffusion-driven growth model is explained by the preferred growth orientation of the mounds grown.

The first author would like to appreciate Professor H. Kaneshiro and Dr. M. Kimura in the University of the Ryukyus for his help and support in use for TEM and AFM.

References

1. A. -L. Barabási and H. E. Stanley, Fractal Concepts in Surface, (Growth,Cambridge Uni. Pr.,1995).
2. F. Family and T. Vicsek, Dynamics of Fractal Surfaces, (World Scientific, Singapore,1991).
3. M. Kardar, G. Parisi and Y. -C. Zhang, Phys. Rev. Lett.,56,(1986)889.
4. Z. –W. Lai and S. D. Sarma, Phys. Rev. Lett.,66,(1991)2348.
5. M. Asanuma and R. Aogaki, J. Chem. Phys.,106,(1997)9938.
6. A. Iwamoto, T. Yoshinobu and H. Iwasaki, Phys. Rev. Lett., 72,(1994)4025.
7. S. Mendez, G. Andreasen, P. Schilardi, M. Figueroa, L. Vázquez, R. C. Salvarezza, and A. J. Arvia, Langmuir,14,(1998)2515.
8. R. K. Pandey, S.N. Sahu and S. Chandra, Handbook of Semiconductor Electrodepositin, (Marcel Dekker,Inc. 1996).
9. F. Family and T. Vicsek, J. Phys. A18(1985)L75.
10. J. G. Amar, P. -M. Lam, and F. Family, Phys. Rev. B, 47(1993) 3242.
11. H. -N. Yang, G. -C. Wang, and T. -M. Lu, Phy. Rev. Lett.,73(1994)2348.
12. J.H.Jeffries,J.-K.Zuo, and M.M.Craig, Phys. Rev. Lett.,76(1996)4931.
13. H. -J. Ernst, F. Fabre, R. Folkerts, and J. Lapujoulade, Phys. Rev. Lett., 72(1994)112.
14. L. Vázquez, J. M. Albella, R. C. Salvarezza, A. J. Arvia and R. A. Levy and Perese, Appl. Phys. Lett.,68(1996)1285.
15. R. L. Schwoebel and E. J. Shipsey, J. Appl. Phys.,37(1966)3682.
16. R. L. Schwoebel, J. Appl. Phys., 40(1968)614.
17. P. Šmilauer and D. D. Vvedensky, Phys. Rev. B,52(1995)14263.
18. J. E. Van Norstrand, S. J. Chey, and D. G. Cahill, Phys. Rev. B, 57(1998)12536.
19. M. D. Johnson, C. Orme, A. W. Hunt, D. Graff, J. Studijono, L. M. Sander, and B. G. Orr, Phys. Rev. Lett.,72(1994)116.

Figure captions

Fig.1 AFM images of the nickel films grown at a low current density of 2mA/cm^2 for (a) 200, (b) 500 and (c) 800sec. Each image size is 2000x2000nm^2 and the vertical scale of each image with a resolution of 512x512 pixels was magnified by a factor of 3.6 in order to enhance viewing.

Fig.2 Log-log plot of the height-difference correlation functions G(r,t) vs r, calculated from the AFM images of the electrodeposited nickel films.

Fig.3 The scaling of the rms roughness w(t) with time, calculated from the AFM images of the electrodeposited nickel films at 323K. The slope of the best fitting line is β=0.78 $\pm$0.03.

Fig.4 Electron and X-ray diffraction patterns of the electrodeposited nickel films. (a) the incident electron beam operated at an accelerating voltage of 160kV was perpendicular to the surface of the nickel film grown for 440sec. (b) the X-ray CuK_α was scattered by the nickel films grown for 1500 sec using a standard θ-2θ diffractometer.

Fig.5 The AFM image of the nickel mounds on the ITO glass that have preferred crystallographic planes. The image size is 500x500nm^2.

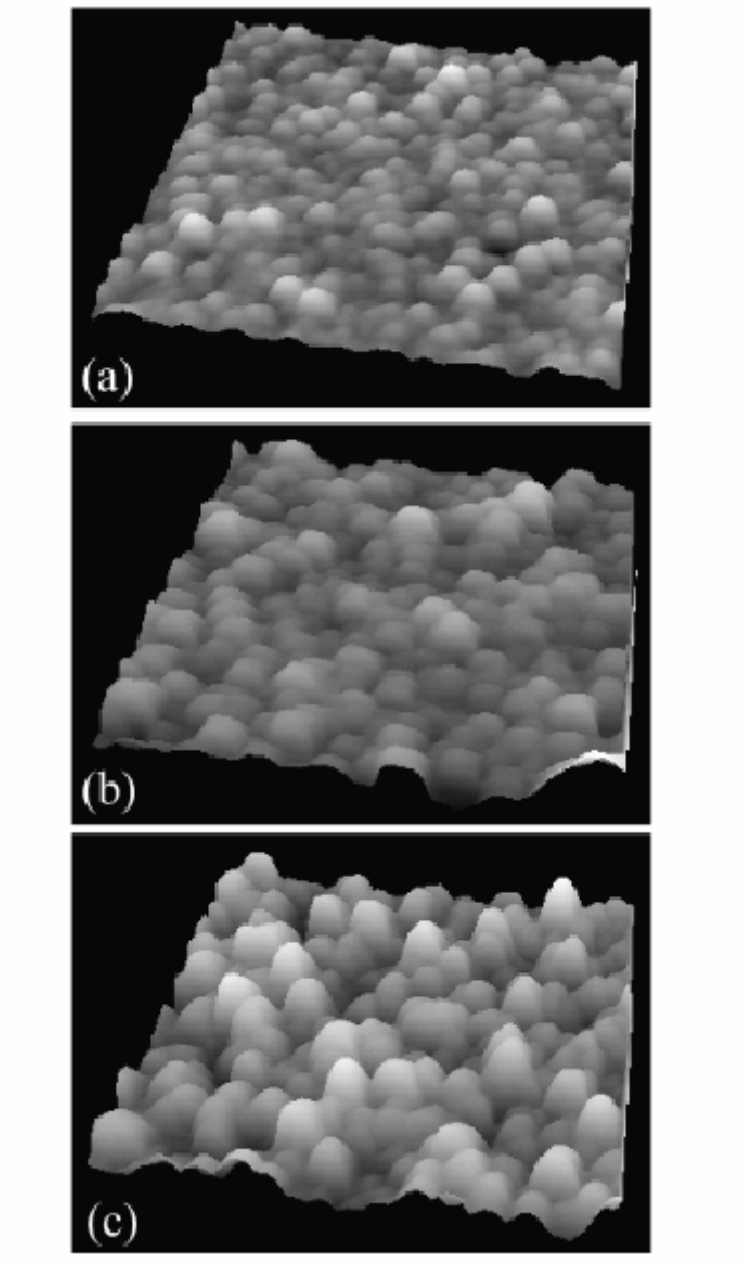

Fig.1 AFM images of the nickel films grown at a low current density of 2mA/cm^2 for (a) 200, (b) 500 and (c) 800sec. Each image size is 2000x2000nm^2 and the vertical scale of each image with a resolution of 512x512 pixels was magnified by a factor of 3.6 in order to enhance viewing.

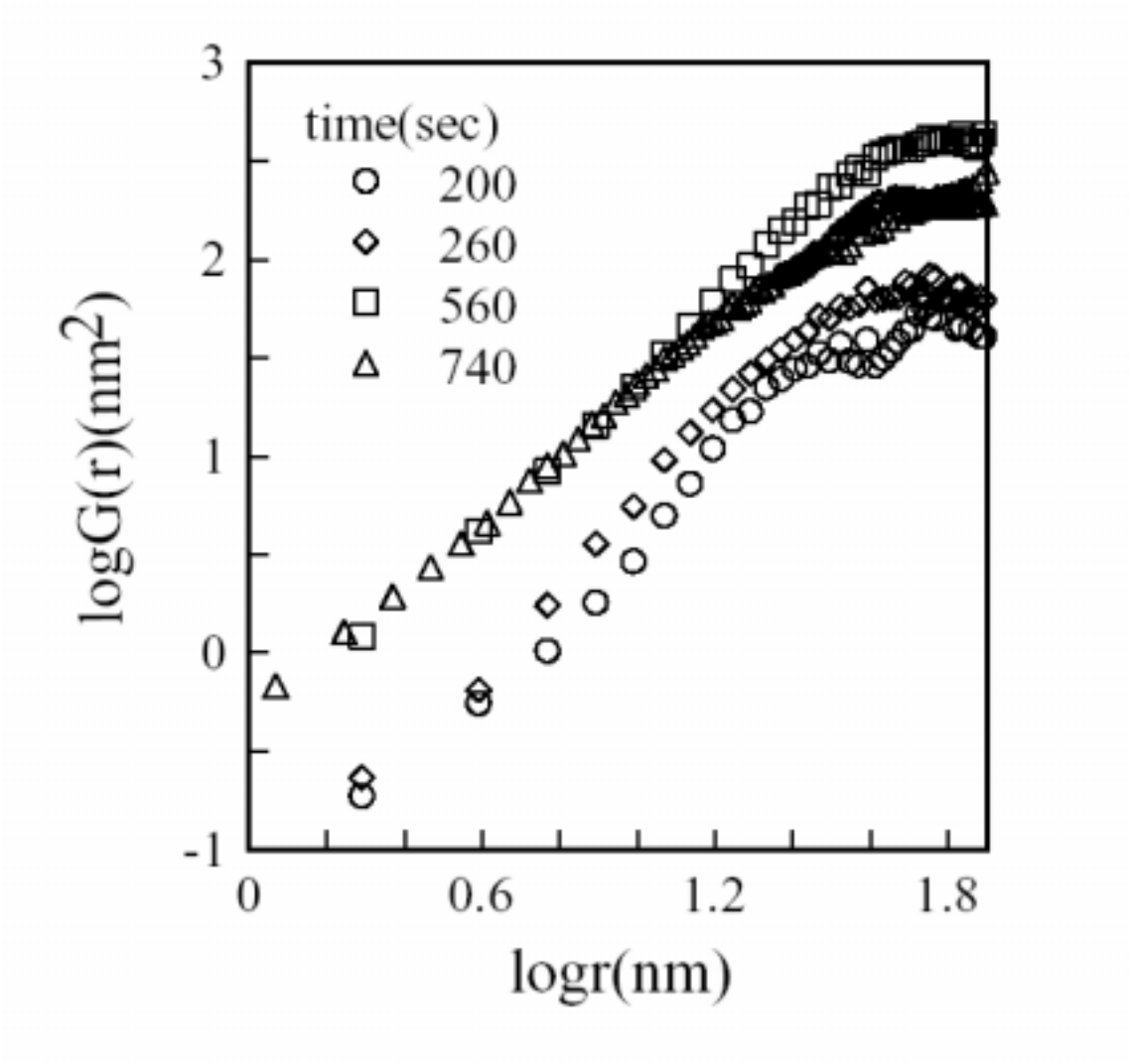

Fig.2 Log-log plot of the height-difference correlation functions G(r,t) vs r, calculated from the AFM images of the electrodeposited nickel films.

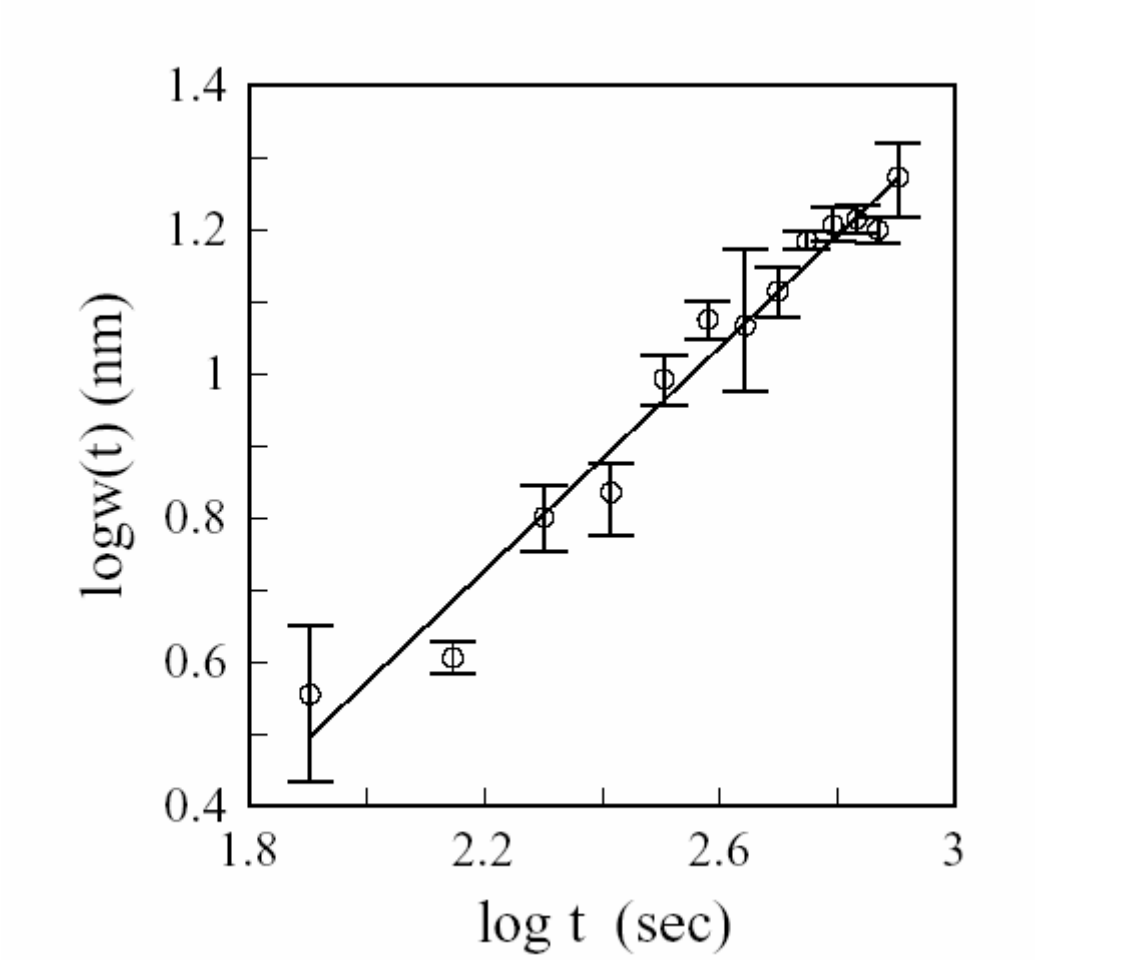

Fig.3 The scaling of the rms roughness w(t) with time, calculated from the AFM images of the electrodeposited nickel films at 323K. The slope of the best fitting line is β=0.78 $\pm$0.03.

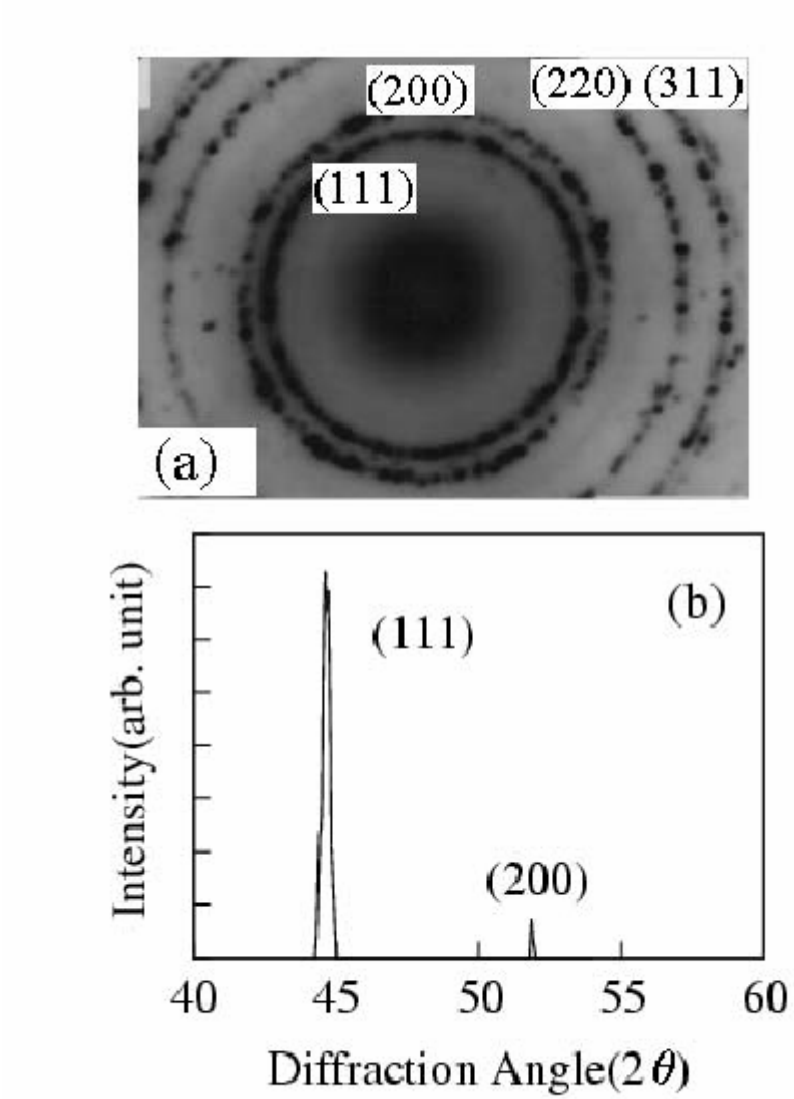

Fig.4 Electron and X-ray diffraction patterns of the electrodeposited nickel films. (a) the incident electron beam operated at an accelerating voltage of 160kV was perpendicular to the surface of the nickel film grown for 440sec. (b) the X-ray CuK_{α} was scattered by the nickel films grown for 1500 sec using a standard θ-2θ diffractometer.

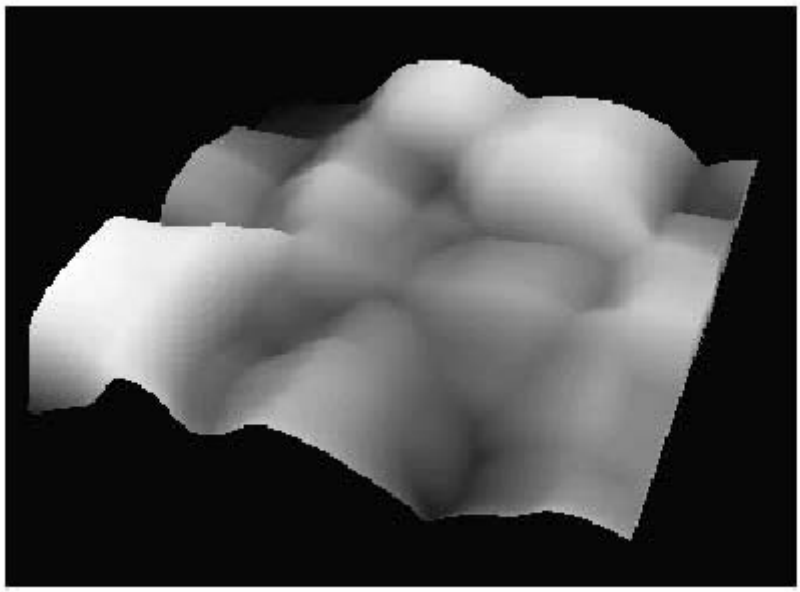

Fig.5 The AFM image of the nickel mounds on the ITO glass that have preferred crystallographic planes. The image size is 500x500nm^2.